California State University, San Bernardino
CSUSB ScholarWorks

Electronic Theses, Projects, and Dissertations | Office of Graduate Studies

10-2023

Early Development of C3aR1-Targeting Chimeric Antigen Receptor T Cells for the Treatment of Glioblastoma multiforme

Cameron Fraser

Follow this and additional works at: https://scholarworks.lib.csusb.edu/etd

 Part of the Biotechnology Commons, Cancer Biology Commons, Cell Biology Commons, and the Translational Medical Research Commons

Recommended Citation

Fraser, Cameron, "Early Development of C3aR1-Targeting Chimeric Antigen Receptor T Cells for the Treatment of Glioblastoma multiforme" (2023). *Electronic Theses, Projects, and Dissertations*. 1823.
https://scholarworks.lib.csusb.edu/etd/1823

This Thesis is brought to you for free and open access by the Office of Graduate Studies at CSUSB ScholarWorks. It has been accepted for inclusion in Electronic Theses, Projects, and Dissertations by an authorized administrator of CSUSB ScholarWorks. For more information, please contact scholarworks@csusb.edu.

EARLY DEVELOPMENT OF C3aR1-TARGETING CHIMERIC ANTIGEN RECEPTOR T CELLS FOR THE TREATMENT OF GLIOBLASTOMA

A Thesis

Presented to the

Faculty of

California State University,

San Bernardino

In Partial Fulfillment

of the Requirements for the Degree

Master of Science

in

Biology

---

by

Cameron John Fraser

December 2023

EARLY DEVELOPMENT OF C3aR1-TARGETING CHIMERIC ANTIGEN RECEPTOR T CELLS FOR THE TREATMENT OF GLIOBLASTOMA

A Thesis

Presented to the

Faculty of

California State University,

San Bernardino

---

by

Cameron John Fraser

December 2023

Approved by:

Nicole Bournias-Vardiabasis, Committee Chair, Biology

Laura Newcomb, Committee Member

Aileen Anderson, Anatomy & Neurobiology-UC Irvine, Committee Member

© 2023 Cameron Fraser

ABSTRACT

Glioblastoma multiforme is the most aggressive type of glioma, demonstrating extremely low long-term survival despite modern therapies. Chimeric antigen receptor T cells have shown extreme levels of success in the treatment of B cell lymphomas through persistent anti-tumor activity. Prior research has demonstrated the therapeutic potential in targeting the C3a-C3aR1 pathway as it acts in an autocrine loop, maintaining the proliferation and survival of cancer stem cells within the tumor. Here, we reorient the treatment to target C3aR1 for the treatment of glioblastoma multiforme. In order to achieve this, Jurkat immortalized T cells will express various chimeric antigen receptor designs through electroporation. We have characterized the initial designs but have not yet generated a construct which definitively activates in the presence of C3aR positive D54-MG cells. An orthotopic xenograft model of D54-MG cells expressing luciferase in NOD-SCID gamma mice was characterized and dose optimized for minimum cell transplant to induce moribund signs at 3-4 weeks post transplantation. These combined results provide a solid foundation for the future in vitro and in vivo experiments supporting the rapid development of novel CAR T cell therapies against glioblastoma.

ACKNOWLEDGEMENTS

I would like to thank the California Institute of Regenerative Medicine (CIRM) for providing the opportunity to work on my M.S. in the field of cell therapies. The CIRM Scholars program and the financial support it has provided has been a boon to my personal and professional success.

I would like to thank Dr. Nicole Bournias-Vardiabasis for making me aware of the CIRM Scholars program and supporting my application and acceptance into the program. It came at a pivotal time in my academic career.

I would also like to thank Dr. Aileen Anderson for accepting me into her lab to work on this project and providing me with the resources and support to produce this work.

Finally, I would like to thank Dr. Laura Newcomb, Dr. Claire Pouget, Dr. Winnie Chan, Dr. John Fraser, Dr. Frank Tufaro, and Kendall Peterkin for their various contributions towards my professional development and general supportive actions.

TABLE OF CONTENTS

LIST OF FIGURES

CHAPTER ONE

INTRODUCTION

Glioblastoma in the Clinic

Glioblastoma multiforme (GBM) is the most common primary malignant brain tumor accounting for approximately 55% of all glioma. GBM has an incident rate of ~3.4 ± 0.51 per 100,000 person-years which roughly translates to 13,000 new diagnoses in the United States each year (Davis, 2018; Dobes, 2011). Those diagnosed with GBM face a poor prognosis with a median survival of only 14-months and a significant reduction in quality of life (QoL). Depending on the location of the tumor, those suffering may experience a variety of neurological disorders. Seizures are common, occuring in 25% of all patients as many as 50% of patients in the later stage of the disease (Moots et al., 1995).

Current treatment for GBM involves an aggressive resection of the tumor followed by radiation and chemotherapy (Davis, 2016). Due to many complicating characteristics of GBM including invasiveness and high rate of recurrence, the survival rate is only 7.6-14.8% at 2-years and 0.6-4.4% at 5-years when treated by maximal resection followed by radiotherapy. The most significant advance in the treatment of GBM has been the introduction of temozolomide (TMZ) to the current standard of care (SOC). This chemotherapeutic agent causes DNA damage specifically in the N-7 or O-6 positions of guanine. The mechanism of action of TMZ is tumor specific as

enzymatic repair of this specific DNA damage is often silenced in tumor cells, though silencing is not a prerequisite for administration of the drug (Jacinto & Esteller, 2007). The inclusion of this drug in the treatment regimen of GBM patients has increased survival to 22-32% at 2-years and 6.4-14.0% at 5-years (Stupp et al., 2009). Regardless, GBM remains incurable and all those afflicted with the disease will eventually experience recurrence. Treatment of recurrent tumors is often more variable and specific to each patient; however, some research suggests that treatment offers no significant improvement in overall survival.

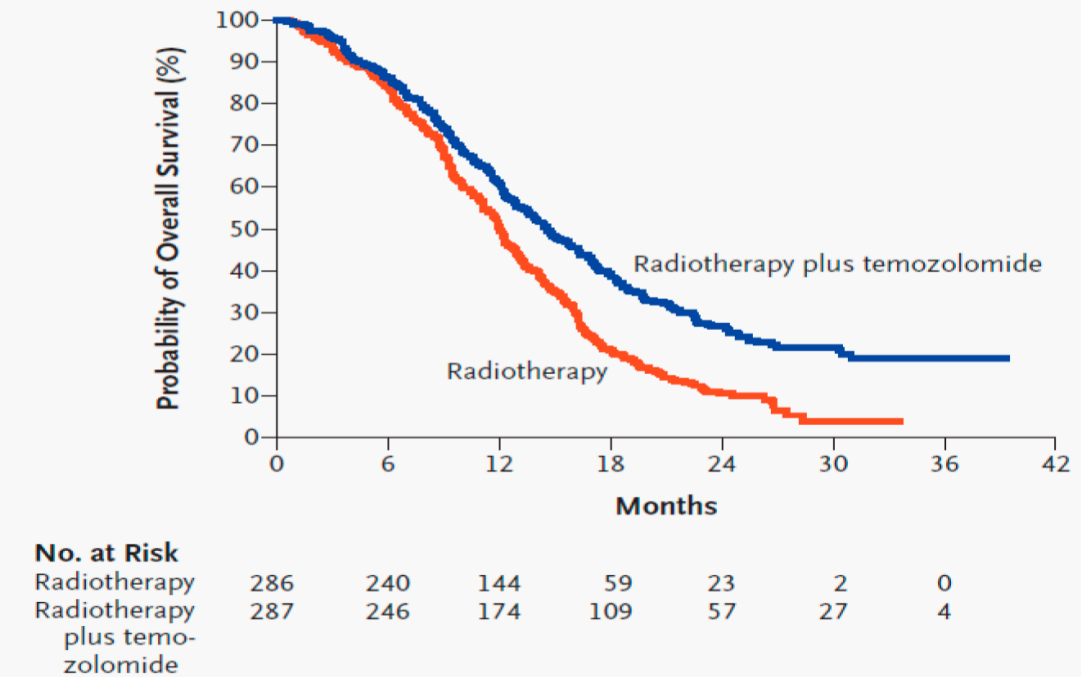

Figure 1: Kaplan-Meyer Curve Representing Impact of Temozolomide. Estimated Kaplan-Meyer curve of GBM patients treated with maximal resection and radiotherapy or maximal resection, radiotherapy, and temozolomide administration. Figure taken from Stupp et al., 2005.

Similarly, clinicians have limited options for symptom management. The most common symptoms considered during treatment are fatigue, cognitive deficits, seizures, depression, and changes in personality (Boele et al., 2014). Patients presenting with seizures are routinely prescribed antiepileptic drugs such as phenytoin. Some studies report that a majority of clinicians, consisting of oncologists, neurologists, and neurosurgeons, prescribed AEDs prophylactically (Glantz et al., 1996). The treatment for other common symptoms varies widely but is most commonly treated by cognitive behavioral therapy. However, this therapy is typically aimed at rehabilitating a patient's QoL by restoring normalcy to their day-to-day lives. For those with relatively little remaining lifespan, this is not necessarily feasible and therefore the typical approach may not appropriately address the patients' specific needs (Boele et al., 2014).

Challenges and Insights from Phase III Clinical Trials

The severity and seeming hopelessness that characterizes the disease continues to drive research both studying characteristics of the disease and developing novel interventions. In the past decade, immunotherapeutic agents have shown significant promise with multiple treatments reaching phase III clinical trials. Immunotherapeutic treatments are not necessarily new, the term broadly describes treatments that manipulate the immune system as their primary mechanism of action. The complex nature of the immune system provides many avenues of manipulation resulting in a wide-ranging array of

treatments. Vaccines are the most public facing category of immunotherapies, but small molecule drugs, immunomodulating proteins, antibodies, and immune cells all fall under the category of immunotherapeutics.

Vaccine based therapeutics showed promise earlier in the rise of immunotherapeutics with DCVax-L and rindopepimut. DCVax-L treatment utilizes autologous dendritic cells that have been pulsed with autologous tumor lysate followed by reinfusion into the patient (Liau et al., 2018). These dendritic cells present antigens from the patient's tumor to T cells which stimulates an anti-tumor response. This treatment is designed to be highly patient specific to maximize efficacy. However, the results of the phase III trial were inconclusive as efficacy was only detected in measuring overall survival (OS), but not progression-free survival (PFS) (NCT00045968). This data was also generated using an external control group generated from the combined results of other GBM clinical trials in which patients received the same SOC with similar patient criteria as the internal control group. Though this was partially taken into account in the analyses, the combined uncertainties throw into question the true efficacy of the therapy (Gatto et al., 2023).

Rindopepimut is a more traditional peptide-based vaccine consisting of a novel amino acid sequence derived from EGFRvIII, a variant of EGFR that is expressed highly on GBM (Sampson et al., 2010). While phase II trial did seem to indicate an improvement in OS compared to the norm (n=66), the follow up phase III trial concluded early after it was concluded that rindopepimut + SOC did

not improve overall survival (NCT01498328, NCT01480479). Notably, while OS in the treatment groups of both phase II and III trials were comparable (~20 months), the control group in the phase III trial had a slightly increased OS (21.1 months) (Malki, 2016). Though some of the disparity in outcomes is thought to be a consequence of the design and methodology of both trials, significant loss of target antigen in the tumor suggests that treatments which target only a single molecular marker may be inadequate for the treatment of GBM (Weller et al., 2017).

Monoclonal antibodies (mAbs) have also shown potential in treating GBM, with researchers probing numerous tumor associated antigens as targets. The vast majority of these have targeted checkpoint inhibitors. The extensively investigated anti-PD-1 therapeutic, nivolumab, has been tested in three different clinical trials indicated for GBM (NCT02017717, NCT02617589, NCT02667587) with variations in patient inclusion criteria and combination with current standard of care (Bausart et al., 2022). However, all failed to reach their primary endpoint. Currently bevacizumab, an anti-VEGF mAb, is the only FDA approved immunotherapy for the treatment of GBM. Even this treatment is controversial as the data from the study only showed improvement in PFS, not OS. Though it has been observed that bevacizumab may also offer improvement in QoL by reducing hemorrhaging resultant from tumor vascularization (Poulsen et al., 2014).

Despite hundreds of clinical trials conducted utilizing diverse and unique approaches, GBM standard of care has remained largely stagnant since the inclusion of TMZ. Similar to many tumors of the central nervous system (CNS), GBM presents as histologically heterogeneous. Indeed, many features of tumors that fall under the category of GBM vary across all levels of granularity. This complicates the development of therapeutics as there will naturally be a prone to variability. Even therapeutics targeting well characterized and common molecular markers for GBM such as EGFR variants, associated with 57% of patients in a multidimensional analysis (n=291), have shown limited in vivo and clinical success (Brennan et al., 2013).

Cell pleomorphism within the tumor also presents difficulty in developing therapeutics. Evidence generated from single-cell RNAseq of 5 different patient samples indicates a wide range of variance in functional phenotype and molecular markers. This includes characteristics such as stemness, state of differentiation, proliferative capacity, and quiescence (Patel et al., 2014). There is evidence in a study assessing GBM vascularization that indicates the capacity of tumor cell differentiation into vascular endothelial cells and pericytes, suggesting a significant role of cancerous cells driving the differentiation of cells, potentially constructing a tumor promoting environment (Cheng et a., 2013; Soda et al., 2011). It can be surmised that this wide variety in cellular characteristics necessitates a treatment that has the capacity for broad targeting while maintaining enough specificity as to not damage non-cancerous cells. Given the

limited success in targeting markers broadly represented in GBM, this approach may be too difficult or inherently flawed. Alternatively, it has been suggested that novel therapeutics that target the entirety of the tumor cell population may be unnecessary when paired with the current standard of care. Instead, targeting the most dangerous subpopulation could be sufficient to suppress recurrence long term.

Glioblastoma Stem Cells

Cancer stem cells (CSCs) were first deliberately isolated and described from a patient suffering from acute myeloid leukemia, though all previously collected and isolated patient samples undoubtedly contained some CSCs in retrospect. These cells newly termed CSCs had the capacity for self-renewal and tumor initiation which seemed to have significant parallels with characteristics of typical, related stem cell populations (Bonnet & Dick, 1997). Since this discovery, CSCs have been discovered and implicated in an assortment of cancers which has consequently led to an expansion and refinement of their definition. Nevertheless, CSCs have been consistently implicated in negative patient outcomes.

In GBM, CSCs have been commonly characterized by co-expression of the stem cell markers CD133 and nestin. Functional comparison of CD133 positive versus CD133-negative tumor cells revealed a correlation between propagation and neurosphere formation (Latia et al., 2015). These glioma stem

cells (GSCs) are associated with tumor resistance to radio- and chemo-therapies (Wang et al., 2021). Analysis of tumor cell compositions revealed an increased proportion of CD133 and nestin positive cells post-irradiation. The implication of GSCs in the progression, recurrence, and treatment resistance of GBM implies that effectively targeting this subpopulation may have a strong impact on patient survival when included with SOC. Still, GSCs present their own unique problems in the development of effectively targeted treatments.

GSCs have an important impact on the tumor microenvironment. Microenvironment refers to the local area in which tumors and GSCs exist, consisting of surrounding immune cells, vascular features, the extracellular matrix, cytokines, fibroblasts, and endothelial cells. All these elements function in a complex interplay which maintains the tumor and suppresses the natural immune response. There is strong evidence to support the important role of GSCs in shaping and maintaining this environment (Prager et al., 2019, Dzobo et al., 2020).

Functionally, GSCs can be classified into two distinct states, quiescent GSCs (qGSC) or proliferative GSCs (pGSC) (Aulestia et al., 2018). While descriptions of subpopulations of quiescent and proliferative GSCs are prevalent in literature, there is no definitive expression profile that distinguishes the two (Lan et al., 2017). Regardless, the presence of functionally diverse GSCs make them difficult to target. qGSCs also operate as a more insidious subpopulation as they can be activated into a proliferative state. This transition is implicated in the

high rate of recurrence unique to GBM. Radiation therapy has also been tenuously connected to this functional transition, though the lack of agreement on the distinguishing features of each cell type leaves uncertainty (Xie et al., 2021).

Engineered T Cell Therapies/CAR T Cells

Amongst other immunotherapeutic approaches, more recently T cells have been singled out for their ability to eliminate cancerous cells. It can be argued that the mechanism of action of conditioned dendritic cell therapies indirectly utilizes anti-tumor T cell activity through APC-T cell cross talk. Earlier attempts at more directly utilizing T cells focused on the isolation, selection, and expansion of tumor infiltrating lymphocytes (TILs) for reinfusion back into the patient. This method, when paired with IL-2 therapy, showed a higher response rate in patients with metastatic melanoma (Rosenberg et al., 1988). Though this treatment approach was marred by logistical and manufacturing issues, it firmly demonstrated the ability of tumor targeting T cells in tackling the problem of solid tumors.

T cell activation through an artificially constructed T cell receptor complex (TCR) was first demonstrated utilizing antibody-derived variable regions targeting phosphorylcholine-positive bacteria (Kuwana et al., 1987). While exciting, this demonstration was to determine the mechanism of antigen recognition by T and B cells. Whether or not these researchers on this project realized the therapeutic potential in their chimeric receptor design is not indicated in their publication.

Though it would not be long until others did. Researchers out of the Weizmann Institute of Science generated a novel receptor that demonstrated non-major histocompatibility-complex mediated activation against a specified target (Gross et al., 1989). The same team would then simplify the design of the chimeric receptor to necessitate only a single-chain of the TCR, eliminating the need for co-transduction with multiple retroviral vectors (Eshhar et al., 1993). While they greatly improved the design of the chimeric construct, they had not yet generated data supporting their supposition that these T cells could be used against tumors.

Instead, a German team would modify the receptor to target ERBB2, a surface receptor that is overexpressed in ovarian cancer. (Moritz et al., 1993). Beyond modifications accounting for antigen specificity, Mortiz's team utilizes the CD3ζ-chain for T cell activation. This construct would become the standard design for the first generation of chimeric antigen receptors (CARs). The anti-ERBB2 CAR T cells not only activated in the presence of ERBB2 expressing tumor cells, but tumor growth was also slowed relative to control treatment in an *in vivo* xenograft model. This phenomenon would be further demonstrated by numerous other studies targeting various cancer subtypes (Weijtens et al., 1996). These early successes *in vivo* prompted the move to generate clinical results.

The first CAR T cell clinical trial was initiated in 1997 for the treatment of ovarian cancer (NCT00019136). Despite supporting *in vivo* data, patients receiving the CAR T cells had no corresponding reduction in tumor burden. This was ascribed to low persistence, as the presence of T cells in the circulation

precipitously declined in all patients two days following infusion (Kershaw et al., 2006). Further development of CAR T cell therapies focused on tackling the problem of persistence from multiple angles.

Second-generation and third-generation CAR T cells are characterized by the addition of the CD28 and CD137 signal transduction domains, respectively (Mitra et al., 2023). These elements were chosen due to their implication in the typical activation of T cells by the TCR. The inclusion of these elements, independently and in tandem, increased T cell persistence and anti tumor activity *in vivo* (Finney et al., 2004). Other deviations from the original trial and CAR design include use of a stronger promoter (EF1α) and a switch to autologous transplant as opposed to allogeneic. Utilizing these characteristics, the National Cancer Institute (NCI) treated a patient in the advanced-stage of follicular lymphoma. Treated with CD19-targeting CAR T cells induced partial remission with very few detectable cells as measured by CD79a immunofluorescent staining of bone marrow biopsies at 36-weeks post treatment. The CAR transgenic sequence was detectable by RT-qPCR from infusion to 27 weeks post treatment (Kochenderfer et al., 2010). This success would be followed up by further trials culminating in the first approved CAR T cell treatment, Kymirah (Maude et al., 2018). The phase III clinical trial that preceded approval demonstrated a rate of remission of 81% at 3 months post-treatment in patients suffering from acute lymphoblastic leukemia (ALL) (NCT02435849). Three more

CD19-targeting CAR T cell therapies would be approved for various B cell malignancies.

To date, a total of 6 CAR T cell therapies have been approved by the FDA for lymphomas and multiple myeloma, each demonstrating impressive rates of remission (Mitra et al., 2023). However, treatment of other cancers has not yet yielded similarly positive patient outcomes. This problem is typically presented as two-fold. First, solid tumors, which represent the vast majority of adult cancers, present significant challenges to the effectiveness of CAR T cell treatment. The immunosuppressive tumor microenvironment associated with solid tumors acts to drive down T cell activation and anti-tumor activity. Second, target selection has proven to be significantly difficult due to tumor heterogeneity, both between patients and throughout each tumor. These specific challenges are both hallmarks of GBM, making it an ideal target to probe for potential solutions that may help to overcome barriers preventing the expanded use of CAR T cells treating the full spectrum of cancers.

CHAPTER TWO

RATIONALE

Evidence produced from previous experiments performed in the Anderson lab have positively indicated the potential of the C3a-C3aR pathway. Patient data from The Cancer Genome Atlas (TCGA) shows a correlation between disease severity and the increased expression of C3aR1 relative to normal tissues. GBM specifically displayed the highest relative expression of C3aR1. *In vitro* data provided supporting evidence for the potential of targeting the C3a-C3aR pathway as the administration of neutralizing antibodies against C3a showed a marked decrease in proliferation and total cell number in patient derived GBM cells. It was further demonstrated that cells with high CD133 expression were targeted and depleted by the treatment, indicating that the treatment acts against GSCs with some level of specificity.

In vivo data utilizing either the neutralizing antibody approach, or the co-administration of C3a and/or C3aR silencing RNA with tumor delivery, demonstrated some impact on survival in a mouse xenograft model. However, these studies were limited by study design as the high initial tumor dose and co-administration of the therapeutic agent may not work as an adequate disease model in which to simulate clinical efficacy.

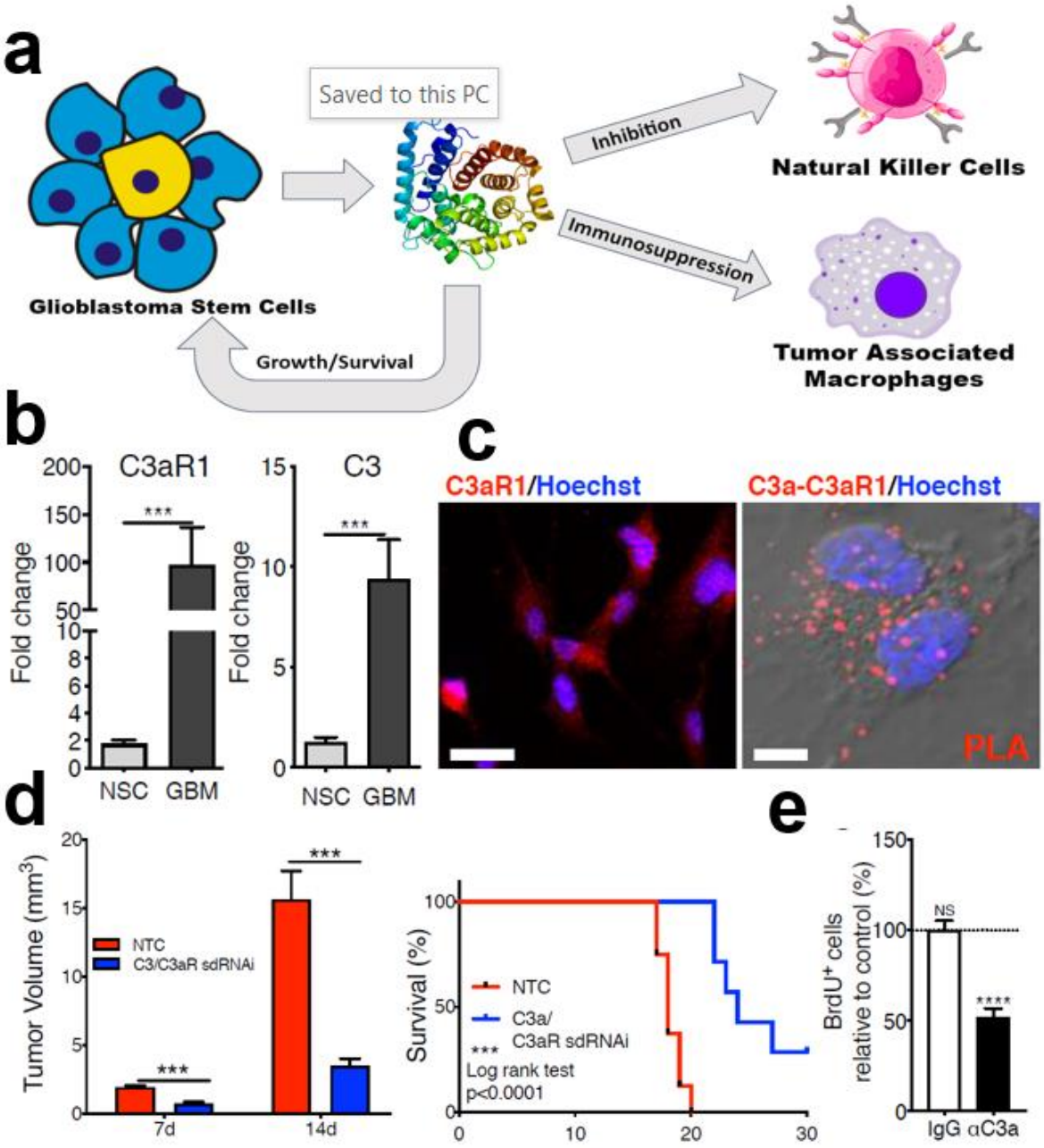

Figure 2: Rationale and Previous Data in Targeting C3aR1. a) Diagram Representing the tumor promoting crosstalk between GSCs and the immune microenvironment with regards to the C3a-C3aR pathway. b) Previous data generated from HuTuP01 GSCs agains human neural stem cells demonstrated overexpression of both C3 and C3aR. c) Immunocytochemistry of the same cell line verified C3aR expression. A proximity ligation assay confirmed interaction of autocrine C3a-C3aR interactions. d) *In vivo* knockdown of the C3a-C3aR pathway by silencing, self-delivering sdRNA interactions lead to decreased tumor volume and increased overall survival in an orthotopic xenograft model. e) Exposure of GSCs to neutralizing anti-C3a mAbs resulted in reduced proliferation measured by BrdU uptake into genomic DNA. Figures b-e were taken from Benavente et al. [Manuscript in preparation].

The treatment approaches themselves are also limiting to the long-term efficacy of the treatment as neither neutralizing antibodies nor silencing RNA have strong capacity for long-term persistence of effect. The lack of long-term persistence has repeatedly tripped up even the most promising attempts at therapeutic development.

To address these issues, this study sets out to further develop and characterize the orthotopic xenograft model as well as apply these early successes in the development of CAR T cells.

CAR T cell development is not an exact science, as there is conflicting evidence for the efficacy of some designs versus other depending on the type of cancer, the source of the antigen binding domain, and other features of the chimeric receptor structure. Therefore, I aim to use a plasmid-based system developed specifically for the rapid generation and testing of different CAR T cell constructs (Bloemberg et al., 2020). I have then optimized the delivery of the plasmid by electroporation of immortalized human T cells for ease in manipulation. I then developed a common assay for the rapid assessment of CAR T cell activation state based on the surface expression of CD69. While initial designs have failed to achieve meaningful activation against GBM compared to controls, this assay will allow for rapid testing of novel constructs developed against the same target.

In accompaniment with the optimization and characterization of in vitro assays, the optimization of the tumor xenograft model in NSG mice was

necessary to improve effect size and timing of treatment delivery. Luciferase expressing D54-MG cells were delivered at varying doses (5e3 - 7.5e4 cells/animal). Tumor progression was then assessed over time by monitoring animal health as well as bioluminescent imaging.

The development of assays and characterization of mouse model will open the doors for the rapid generation and testing of novel CAR constructs that is necessary in efficiently producing a functional and efficacious treatment.

CHAPTER THREE

SPECIFIC AIMS

Aim 1: Generate Multiple C3aR1 Targeting CARs

Rationale

While the mechanism of action of chimeric antigens receptors is relatively well understood, there is a great need for optimization when approaching novel targets. A multitude of factors impact the function of CAR T cells requiring fine tuning of the design. This includes affinity to target antigen as well as the accessibility of the antigen to the receptor.

Approach

To address this, the single chain variable regions of two different clones of C3aR1 targeting antibodies have been implemented in the chimeric antigen receptor designs. These antibody fragments were joined by a short space peptide and anchored to the cell membrane by the CD28 transmembrane region. The corresponding cDNA sequence for this portion of the CAR was cloned into a anti-CD19 CAR expressing plasmid to retarget the total construct.

Aim 2: Optimize the Method for Characterization of CAR-T Cells

Rationale

Discriminating between the magnitude of activation of variations of C3aR1 targeting CAR constructs necessitates a sensitive, reproducible assay, and

economical assay. Developing this assay will build off of the methodology described by Bloemberg et al. (2020). Jurkat cells, a well characterized CD4+ T cell line, will be electroporated with CAR construct containing plasmids for transient CAR expression. Measuring activation will employ the use of flow cytometry to measure the relative expression of CD69, a common T cell activation marker, when challenged against target cells. D54-MG cells will be used as target cells as they have been previously used in our lab to demonstrate changes in C3aR1 expression under various conditions. Raji B cells will be used as a positive control for activation when co-cultured with CD19-targeting CAR T cells.

Hypothesis

T cell activation state of Jurkat cells which transgenically express C3aR targeting CARs will differ between monoculture and D54-MG co-culture conditions.

Approach

Transfected T cells will be co-cultured with D54-MG cells at effector:target ratios of 100:1, 10:1, 1:1, or 1:0 as well as 1:1 with Raji cells. Following 24 hours of co-culture, cells will be stained with fluorescently conjugated αCD3, αCD45, αCD69 antibodies. T cells will be discriminated from target cells by size as well as the co-expression of CD3 and CD45. CAR expressing T cells will be discriminated by the positive expression of GFP when compared to a relevant control condition. Activation of CAR T cells will be quantified by the mean

fluorescent intensity of αCD69 fluorophore in GFP+ T cells. This base methodology will be adapted as necessary to suit the specific needs and challenges of our specific experiment.

Aim 3: Characterize and *in vivo* Model for Testing CAR-T Cells

Rationale

Once a strong candidate C3aR1 targeting CAR construct is identified using *in vitro* techniques, *in vivo* testing will be performed to obtain a more accurate indication of efficacy. Previous attempts at developing C3a-C3aR targeting immunotherapeutics in our lab have shown positive indications of efficacy, however the results are limited due to study design. Effect was only measured when treatment was delivered at the same time point as tumor xenograft surgery. We theorize that this phenomenon is due to the initial high tumor dose which provides a hindrance to efficacy that is not representative of GBM pathology in patients. Therefore, we sought to generate data to support future studies in which tumor dose may more accurately mirror clinical GBM, while still producing lethal effects in untreated mice prior to the anticipated onset of confounding innate immunological responses to either tumor or T cell xenografts.

Hypothesis

Differing doses of tumor cells engrafted into the cerebrum of NSG mice will produce significant differences in survival, tumor volume, and tumor morphology.

Approach

To ensure a rapid turnaround, the GBM mice model will be optimized concurrently with *in vitro* testing. D54-MG cells modified to express luciferase will be transplanted into immunodeficient Nod scid gamma (NSG) mice at various concentrations. Luciferase expression will be monitored over time using live animal imaging to measure tumor growth. Mice will be monitored for pre-defined criteria for euthanization. The day of euthanization post-surgery will be the primary metric for determining optimal cell dose to obtain a positive signal for CAR T cell antitumor function while mitigating the impact of graft-versus-host disease.

CHAPTER FOUR

MATERIALS AND METHODS

Chimeric Antigen Receptor Design

The original CD19 targeting CAR plasmid construct was sourced from AddGene and generated by Dr. Darin Bloemberg (2020). Cloning using this plasmid requires the generation of a unique C3aR1 targeting CAR construct containing the signal peptide, antibody single chain variable regions, and hinge region. The signal peptide consists of the human CD28 signal peptide (aa 1-18, NP_006130.1). The single chain variable regions consist of the variable heavy chain and variable light chain from either the 2A1 or 3G7. The sequences were sourced from the Antibodies Chemically Defined Database (ABCD). The variable regions were oriented in the VL-VH configurations and connected using a unique linking peptide (GSTSGSGKPGSGEGSTKG). The final portion of the fragment consists of the first peptides of the human CD28 transmembrane domain. This construct contains cut sites for the BpiI type IIS restriction enzymes.

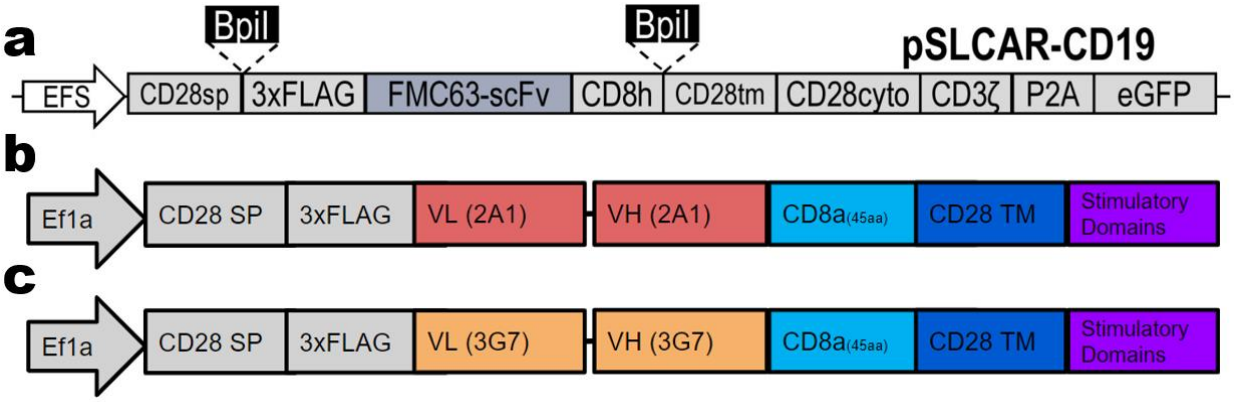

Figure 3. Plasmid Maps of Traditional and C3aR1 Targeting CARs. a) The pSLCAR plasmid with the proper restriction enzyme sites (BpiI) for the cloning of different CAR constructs. The Ef1a promoter drives strong, constant expression of the CAR. The 3X FLAG sequence is commonly used in order to perform immunostaining for the presence/localization of CAR expressing cells. The monoclonal antibody variable fragments from either clone 2A1 (b) or clone 3G7 (c) were oriented in the VL-VH orientation. This region is appended by the CD8 derived hinge region. The receptor is anchored to the cell membrane by the CD28 transmembrane domain. The intracellular domain is composed of the classic 3rd generation CAR constructs (CD3-zeta chain, CD28 stimulatory domain, 4-1BB stimulatory domain).

Plasmid Cloning Procedure

The complete C3aR1 targeting CAR containing plasmids were generated using a single reaction mixture containing BpiI restriction enzyme, T4 ligase, T4 ligase buffer, pSLCAR-CD19 BBz plasmid, and the C3aR1 targeting CAR gene fragment. Following the one-step digestion-ligation reaction, the resultant plasmids were incubated with DH5α competent E. coli cells. Transformed bacteria was plated for clonal selection. Selected colonies were expanded in LB broth containing ampicillin. Plasmid isolation was performed using MiniPrep kits

according to the manufacturer protocol (Qiagen). Plasmids were screened by PCR using C3aR1 targeting CAR specific primers.

Cell Lines and Culture Conditions

Human CD4+ T (Jurkat E6.1) cells were sourced from Dr. Wein Zhao. Stable B cells (Raji) were sourced from ATCC. Jurkat T cells and Raji B cells were maintained in RPMI 1640 medium (Gibco) supplemented with fetal bovine serum in non-tissue culture treated flasks. Stable human glioblastoma cells (D54-MG) were a gift from Dr. Darrell Bigner (Duke University, Durham, NC). Luciferase expressing D54-MG cells were generated by Dr. Fransesca Benevette using lentiviral transduction. HEK-293 cells were cultured for downstream lentivirus generation. D54-MG, D54-MG Luc, and HEK-293 cells were maintained in DMEM (Gibco) supplemented with fetal bovine serum in tissue culture treated flasks.

Electroporation of Jurkat Cells

Jurkat cells were transfected by electroporation using a Lonza Nucleofector I and program X-01. Electroporation cuvettes and 1M buffer (1M

5mM KCl; 15mM MgCl2; Na2HPO4/NaH2PO4; 50mM Manitol [pH 7.2]) was chilled on ice prior to electroporation. The optimal Cell:DNA ratio was determined to be 1µg of plasmid per 10^5 cells. According to this ratio, the appropriate volume of purified plasmid is prepared in 1M buffer to a total volume

of 100µL. The corresponding number of cells are then resuspended in this buffer mixture and then applied to an electroporation cuvette. The cuvettes are then allowed to sit at room temperature for approximately 2 minutes before running the nucleofector. The cells are then placed back on ice for approximately 2 minutes prior to the addition of 500µL of pre-warmed recovery medium (RPMI 1640 + 20% FBS). Transfected cells were then plated out into recovery medium and incubated at 37°C for 4 hours.

T Cell Activation Assay

D54-MG cells were plated into a 96-well plate in varying cell concentrations (3e4, 3e3, 3e2 cells per well) in RPMI 1640 medium + 10% FBS. Raji cells were also added to the plate at a concentration of 3e4 cells per well as a positive control for activation of the CD19 targeting CAR. Jurkat cells were dosed with CD3/CD28 T Cell Activating Dynabeads to artificially stimulate activation to act as a positive control (Gibco, NY, USA). Following incubation, transfected Jurkat cells were applied to the appropriate wells and returned to 37°C incubation for 24 hours.

Jurkat activation was measured using flow cytometry for the expression of CD69, a common T cell activation marker. Cells were stained in the wells using APC-conjucated anti-CD69 (Becton Dickinson, BD #555533), BV786-conjugated anti-CD3 (BD #566781), and PECy7-conjugated anti-C3aR1 (BioLegend, Cat. No 345808) antibodies. Antibodies were allowed to incubate for 30 minutes at 37°C.

The plate was immediately analyzed on a BD Fortessa X-20 flow cytometer. T cell activation was quantified by the mean fluorescent intensity (MFI) of the APC channel.

Determination of Optimal D54-MG-Luc Dose in NSG Mice

A dose range of 5,000 to 75,000 was determined to be appropriate in order to establish the optimal dose to achieve approximately 21 days of survival in NOD-SCID gamma mice. D54-MG-Luc cells were collected and resuspended in 0.22µm filtered, unsupplemented DMEM to varied final concentrations that correspond to the cell dose range for 1µL total injection volume. The cell suspension was then loaded into the syringe of an automatic injection system. NSG mice (N=3 per dose group) were injected with the cells at a spot 2 mm left of bregma and 1 mm anterior to coronal suture.

Tumor growth was evaluated using bioluminescent imaging utilizing the Xenogen IVIS Lumina Animal Imaging System (PerkinElmer, Santa Clara, CA, USA). Luciferin diluted in sterile PBS was injected into the intraperitoneal cavity of each mouse approx. 10 minutes prior to imaging. Images were taken over a time-course of 25 minutes at 5 minute intervals for a total of 6 images of each mouse per time point. Tumor burden was assessed using mean total flux measured using Living Image software.

Mice were monitored daily for moribund signs. Mice that met predetermined criteria of moribund signs were sacrificed immediately. The brains

were collected and fixed in a solution of 4% PFA and 20% sucrose. Following fixation, the brains were frozen and saved for future analyses.

Histology

Cryopreserved brains were embedded in NEG50 (Epredia, MI, USA). 30 µm thick coronal sections were cut using a cryostat and sections mounted using a CryoJane tape transfer system (Leica Biosystems, Inc., Buffalo Grove, IL). A section interval of 1/24 was utilized, placing adjacent sections analyzed at 720µm apart. Tissue slides were heated to 60°C for 45 minutes for antigen retrieval. Tissue was then rehydrated prior to hematoxylin and eosin (HE) staining. Tissue was briefly submerged in a hematoxylin solution and then rinsed with water. Tissue sections were then submerged in a differentiation solution composed of 70% EtOH and 10mM acetic acid for approx. 1 minute. Tissue sections were then submerged in a 0.5% Eosin Y staining solution for approx. 15 seconds before rinsing with water (Sigma-Aldrich). Tissue sections were then dehydrated, mounted and stored for imaging.

Tumor volume was quantified using Stereoinvestigator software (MBF Bioscience, USA). Tumors were assessed at 4X magnification. Tumor volume in HE slices was quantified using the following formula (Gundersen et al., 1987), where V is estimated volume, AP is area associated with a point, m is section evaluation interval, t is mean section cut thickness, Pİ is points counted on grid. These applications were performed on all slices of each subject. Section

thickness was set to 30µm and section evaluation interval was set to 720µm. An overestimation compensator was applied to the final volume calculations to generate the most accurate tumor volume. One subject in the 5k group was excluded from volume estimation due to significant tissue loss during cryostat sectioning.

CHAPTER FIVE

RESULTS

Aim 1: Generation of Chimeric Antigen Receptor Constructs

Gene fragments for CAR constructs were obtained from Integrated DNA Technologies (IDT) and cloned into the base CAR vector plasmid. Successful integration of the clone was determined by PCR amplification using construct specific primers as well as the use of an analytic restriction enzyme digest (Figure 2). A restriction enzyme site is lost as a result of insert integration, therefore only the vector plasmid should reveal two distinct bands when separated by gel electrophoresis. Using this technique all cloned plasmids (e-l) showed only single bands whereas the unmodified vector plasmid (a-d) showed two distinct bands. Successful cloning was further verified by sequencing candidate plasmid samples.

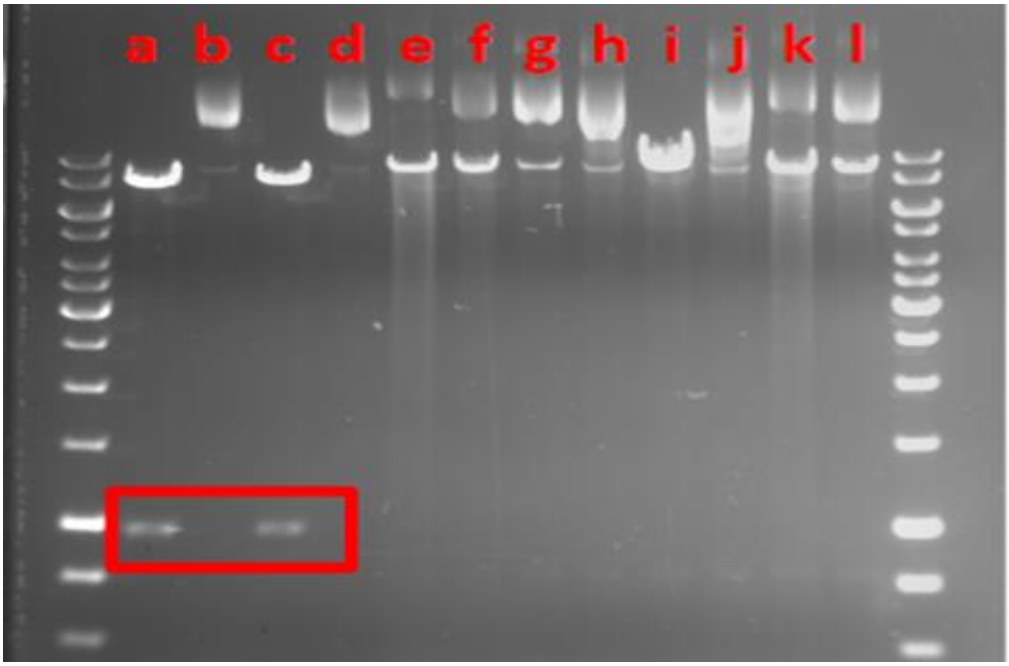

Figure 4. Restriction Enzyme Digest of Cloned Plasmids. Restriction enzyme (RE) digestion was performed with BpiI. Samples a-d are unmodified CAR vector. Samples e-l are modified C3aR1 CAR constructs. Samples alternate in RE treatment and no treatment from left to right. The unmodified vector digests were the only samples to resolve two distinct bands.

Aim 2: Optimization of Characterization of CAR-T Cells

Optimization of Jurkat Electroporation

Jurkat electroporation required optimization in procedure, materials, and determining cell:DNA ratio. The use of a commercially available kit did not yield any significant percentage of transfected cells compared to the control as measured by positive GFP expression. Based on a literature search as well as a review of troubleshooting documents from Lonza, New England Biosciences, and other producers of electroporation reagents, numerous specific aspects of the

protocol needed modification. It was speculated that the primary difficulty in transducing cells is the size of the transfecting plasmid (9kb) (Chicaybam et al., 2017).

The procedure was optimized to include pre-chilling of the electroporation cuvettes and nucleofection buffer. The buffer provided by a commercial kit was also substituted with a buffer described in Chicaybam et al. (2017). The final procedure and use of the 1M buffer yielded successful expression of GFP in Jurkat cells. Further optimization was performed to establish an ideal concentration of plasmid. Analysis by flow cytometry of the population of cells showed that 6µg per 600,000 cells yielded the greatest portion of GFP expressing cells (25.9%; Figure5c).

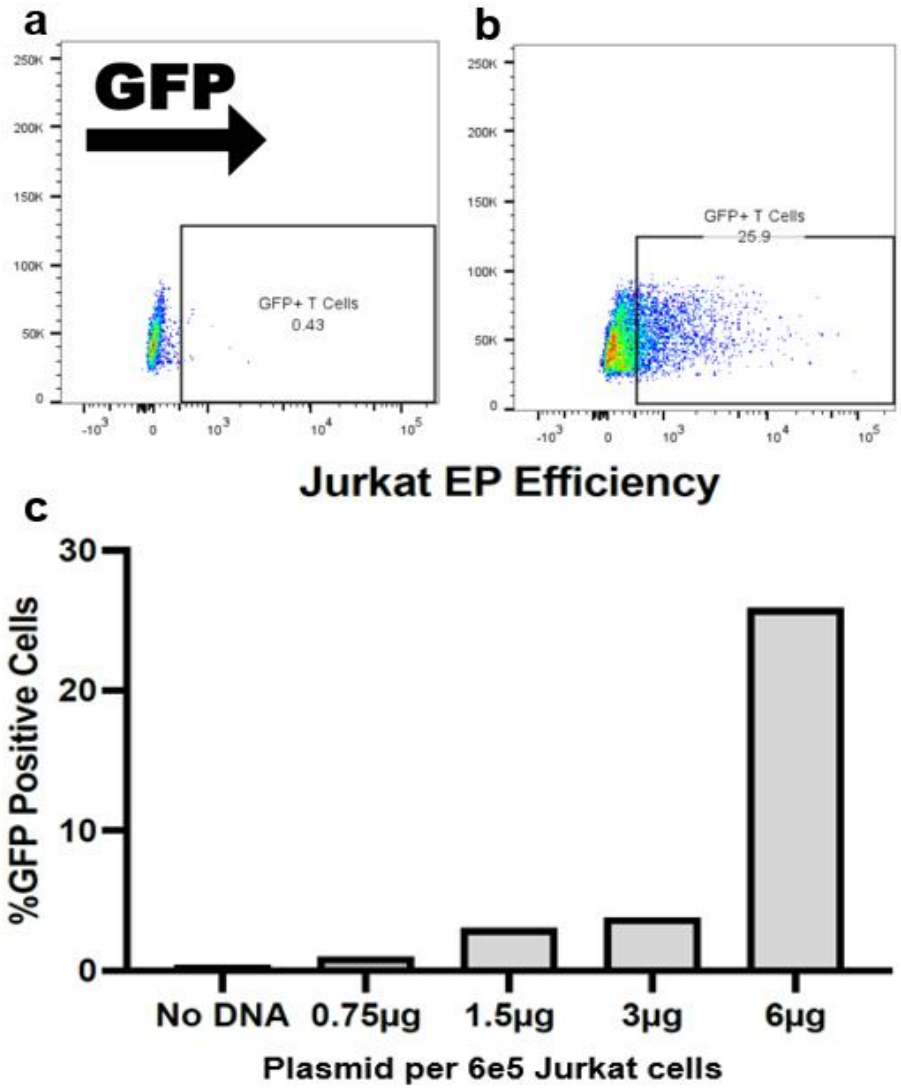

Figure 5. Flow Cytometric Analysis of Optimized Electroporation. a/b) The gating strategy utilized to assess positive GFP expression. Negative control for GFP expression were T cell that were subject to electroporation without any addition of plasmid as electroporation resulted in low levels of autofluorescence. c) Increasing amounts of plasmid resulted in a greater proportion of cells expressing the pSLCAR trangenes.

CAR-T Cell Co-Culture with D54-MG Cells

The mean fluorescent intensity capture of GFP+ Jurkat cells in the APC channel was collected from the BD Fortessa X20. Co-culture of anti-C3aR targeting CAR T cells with D54-MG cells showed an apparent inverse relationship between the number of target cells and APC MFI, though this trend was not statistically significant. All constructs, both targeting CD19 and C3aR, demonstrated activation in response to co-culture with Raji cells. CD19 targeting CAR T cells exhibited the highest level of activation, though all activation was statistically significant ($p = 0.047, 0.002, 0.011$ respectively).

This result was repeated in a following experiment in which both C3aR targeting CAR T cells were cultured with two different quantities of Raji cells (Figure 6b). Activation was observed in a dose dependent manner for Raji cells. Some activation was also observed in naive T cells in a similar dose dependent manner.

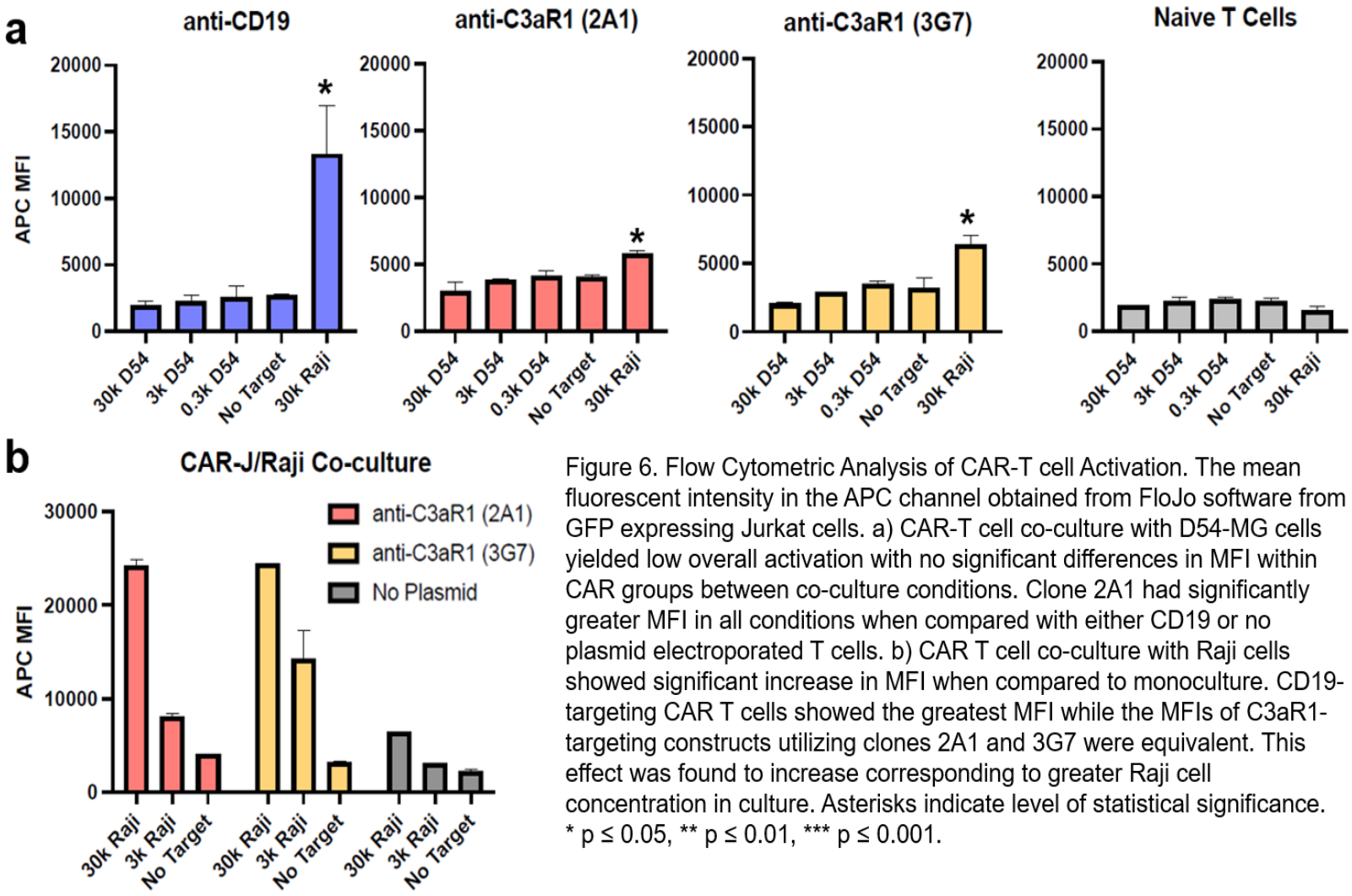

Figure 6. Flow Cytometric Analysis of CAR-T cell Activation. The mean fluorescent intensity in the APC channel obtained from FloJo software from GFP expressing Jurkat cells. a) CAR-T cell co-culture with D54-MG cells yielded low overall activation with no significant differences in MFI within CAR groups between co-culture conditions. Clone 2A1 had significantly greater MFI in all conditions when compared with either CD19 or no plasmid electroporated T cells. b) CAR T cell co-culture with Raji cells showed significant increase in MFI when compared to monoculture. CD19-targeting CAR T cells showed the greatest MFI while the MFIs of C3aR1-targeting constructs utilizing clones 2A1 and 3G7 were equivalent. This effect was found to increase corresponding to greater Raji cell concentration in culture. Asterisks indicate level of statistical significance. * $p \leq 0.05$, ** $p \leq 0.01$, *** $p \leq 0.001$.

Aim 3: Characterization of *in vivo* Model for Testing CAR-T cells

All animals successfully survived xenograft surgery. Throughout the duration of the experiment, no significant health aberrations were observed in any of the subjects. Tumor growth was observable by bioluminescent imaging in all groups starting from day 10 post surgery. Tumor growth was assessed regularly by bioluminescent imaging throughout the duration of the study. Subjects dosed with 2.5e4, 5e4, and 7.5e4 cells rapidly declined in health at approximately day 21 post surgery. Subjects within these groups were sacrificed between days 22 and 26 post surgery according to predetermined criteria for euthanasia (Figure 7b). With the exception of a single subject, animals in the lower dose groups (5e3 and 1e4 cells per animal) declined through week 4 post surgery, achieving criteria for euthanasia at days 34 and 35 post surgery. The mean survival time for all animals decreased with increased dose of D54-MG cells.

Bioluminescent imaging of the tumors showed an exponential growth curve for all dose groups. Higher dose groups achieved a maximum signal of 4.52e8 ph/s (± 0.51e8; 95% CI) at the last acquisition before euthanasia (D22 post-surgery). Tumors in the lower dose groups at this same time point measured approximately half of that signal (~2e8 ph/s). Lower dose animals survived longer, however, and subsequent bioluminescent imaging measurements continued to increase exponentially, reaching a peak measurement of 5.81e9 ph/s (Figure 7c).

Brain tissue collected and processed following euthanasia revealed the extent of tumor growth in each dose group. The results formed a bimodal distribution in which the greatest tumor volume at the time of sacrifice was observed in the 5k and 75k groups (165mm^3 and 76 mm^3 respectively). However, these groups also demonstrated high variation between animals (Figure 7d). The tumors were observed to occupy a significant portion of the brain causing damage to surrounding tissues.

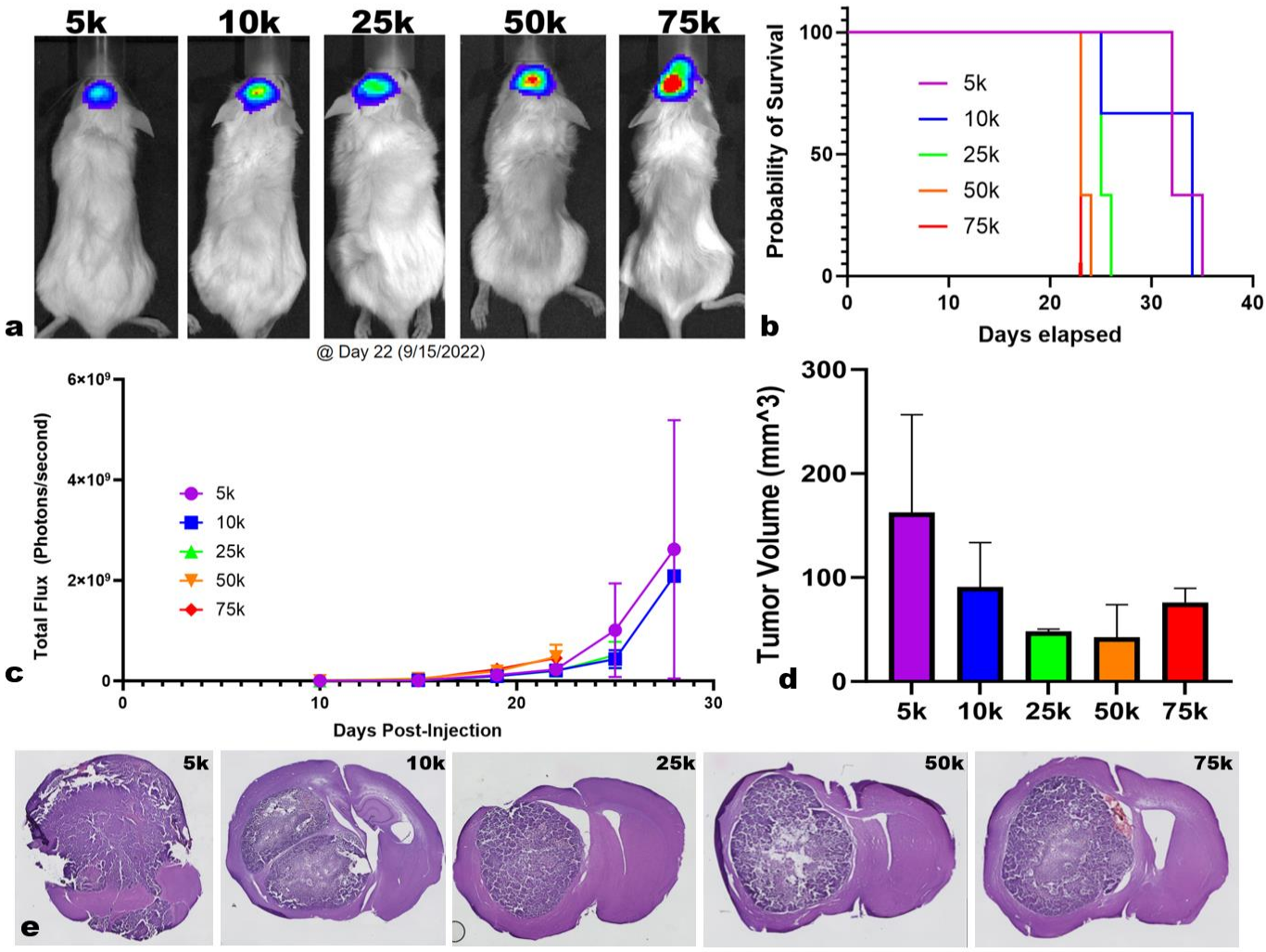

Figure 7) Multiple Analyses of Tumor Volume. a) Representative images of the mice at each dose group on day 22 post surgery. Though there was significant variation within and between groups, bioluminescent intensity increased with dose group when averaged. b) Survival curves showed rapid decline of high dose groups between days 22-26 post surgery. Lower dose groups would decline more gradually in the following 2 weeks. c) Bioluminescent measurements show exponential growth measured by photon emission resultant of luciferase-luciferin reaction. d) Tumor volume assessed by histological analysis of cryopreserved brains. e) Representative images of stained brain sections containing tumors of various sizes. These sections were selected from sections in roughly the middle of the tumor to approximately display volume.

CHAPTER SIX

DISCUSSION

The generation of the desired CAR constructs was successful, indicated by PCR and restriction enzyme digests. The optimization of transfection of the Jurkat cells was successful, with a high percentage of GFP expressing cells when compared to those seen in Bloemberg et al. (2020). Though further conditions could be tested, further optimization would likely yield marginally improved results that would not significantly impact the downstream application of characterization assays. Instead, the literature supports using *in vivo* models to more rigorously test the potential efficacy of novel CAR-T cells.

Both C3aR constructs failed to achieve D54-MG directed activation of transfected Jurkat cells. Alternatively, the activation state of the T cells was inversely proportional to the number of D54-MG cells in culture. While this trend was not statistically significant, the consistency of the trend between conditions could indicate an inhibition of activation mediated by D54-MG cells. It is known that cancers, in particular GBM, act to suppress anti-tumor immune response,

Surprisingly, the C3aR targeting CAR T cells showed statistically significant activation when cultured with Raji B cells. This phenomenon was originally thought to be an artifact of the known interactions between T cells and B cells which may induce activation. Indeed, this was observed in co-culture conditions containing naive T cells and Raji B cells, even demonstrating a dose

dependent effect. However, this activation, measured as CD69 expression measured by flow cytometry, was much lower than activation achieved by both CAR T cell constructs. It is highly unlikely that this weaker activation seen in the C3aR1 constructs is a result of error during cloning as the process is rigorous to produce plasmid stocks containing single clones. Screening of these stocks also shows no indication of the presence of substantial amounts of base CD19-targeting CAR plasmids. Further investigation to conclusively quantify C3aR1 protein in both Raji and D54-MG cells under different conditions is necessary. Similarly, knockdown or knockout of C3aR1 expression in Raji cells would provide evidence of C3aR1-targeting constructs activating against a non-C3aR1 antigen. Many published *in vitro* assessments of CAR T cell function utilize target cells that have been transgenically modified for high expression of their target using strong promoters such as Ef1α or CMV (Bloemberg et al., 2020; Tang et al., 2019; Ravanpay et al., 2019). This approach may be implemented for the initial *in vitro* screening of candidates to gain greater resolution in function as well as improve CAR design that may be tested downstream against primary GBM cells. Work to generate and validate a suitable cell line by screening may be more suitable is ongoing.

In any case, the generation of CAR T cells which function strongly against GBM cells *in vitro* will eventually necessitate a robust *in vivo* model. Our orthotopic xenograft model is fairly standard amongst GBM studies, however dose titration is necessary as different cancer lines have different capacities for

proliferation, invasiveness, and survival which all can contribute towards different survival times and other relevant treatment outcomes.

Survival time of subjects within dose groups was as anticipated, with significant differences between survival curves of each group ($p = 0.0008$; Mantel-Cox test). The mean survival times of each animal decreased consistently with cell dose as expected. Bioluminescent intensity measurement of different dose groups tended to separate into “low” and “high” dose groups. The high dose groups, consisting of those subjects receiving 50k and 75k D54-MG cells, while the cluster of lower dose groups were 5k, 10k, and 25k. This resolved differently in survival, as the 25k dose group reached symptomatic criteria for euthanasia around week 4 post surgery similar to 75k and 50k dose groups.

Histological analysis of the tumor volumes showed a bimodal distribution in which the lowest and highest dose groups have the largest tumors at the time of sacrifice. While it was unexpected that the lower dose groups would be burdened by such large tumor volumes, it correlates with the bioluminescent data collected, where the lower dose groups progressed to produce exponentially greater radiance values compared to high dose group values at their final time point prior to euthanasia. These combined results suggest tumor volume remained relatively low in low dose groups when compared to higher dose groups allowing for prolonged survival, yet that survival in turn allowed for exponential growth at later time points.

Our dose titration has provided valuable data which will contribute not only to future CAR T cells, but the development and testing of other similar immunotherapeutic treatments. One limitation of developing CAR T cell therapies in xenograft tumor models is the incidence of graft-versus-host disease (GvHD). GvHD describes an immune reaction by the allogeneic T cells against host mouse cells. While the CAR directs T cell activation against a specific target, unless there is a more complex genetic manipulation of the modified T cells, they will also perform their natural function to activate against non-self cells (Negrin & Contag, 2006). This can be a confounder in performing *in vivo* experiments as GvHD can cause severe liver damage, skin, and gut mucosa and can eventually result in subject death. Therefore, making a determination of the progression of the tumors and anticipated time of death in each dose group allows for selection of a dose dependent on the design of different studies. Timing of both tumor and T cell injection can be optimized to reduce the impact of GvHD while maximizing the power of the experiment.

CHAPTER SEVEN

FUTURE DIRECTIONS

Development of novel CAR T cell therapies is often preceded by approaches using monoclonal antibodies against the same target. Through this process, antibodies are developed and then characterized for binding affinity and functional anti-tumor effect. This refinement paves the way for a functional CAR construct utilizing the variable regions of the most promising monoclonal antibodies. Indeed, this timeline of development was utilized to derive the variable regions used in the construction of CD19 targeting, FDA approved CAR T cell constructs (Zola et al., 1991). Therefore, given the lack of evidence supporting functional activation of either the 3G7 or 2A1 based constructs, resorting to the initial development of therapeutic antibodies as a known approach seems a sensible next step.

This necessitates the development of hybridoma specific for C3aR. While modern techniques for hybridoma development typically utilizes purified target protein for immunization, I believe that this approach is suboptimal for the development of cancer targeting therapeutics and specifically those targets with significant membrane bound regions. cell-based immunization is evidently effective at producing therapeutically qualified mAbs. Moreover, this approach offers advantages both generally and specifically to the generation of C3aR1 targeted antibodies. First, this method avoids the burden of acquiring large

quantities of isolated protein. Second, antigens are presented in their natural conformation at the cell surface. This is particularly useful in targeting C3aR1 is a G protein coupled receptor with multiple intracellular/extracellular loops. A recombinant protein-based approach risks conformational differences resulting from lack of a membrane as well as the production of antibodies that target intracellular regions. Alternative recombinant protein approaches might use fragmented protein, immunizing with only extracellular portions of the protein which also risks conformational changes. Third, the same cell line generated for immunization can be utilized to perform high throughput screening based through flow cytometry. This process should yield a workable number of C3aR1 targeting mAb producing hybridoma lines from which a suitable candidate mAb can be sourced for the construction of a functional and robust CAR construct.

When completed, proven C3aR1-targeting CAR constructs will not only provide evidence of the potential of this antigen, but also be a platform for the design of more complex and robust CAR constructs. The current state of research into modified T cells for cancer treatment has far surpassed 3rd generation, single target CARs (Jayaraman et al., 2020). Bispecific CAR T cells can both broaden targeting capabilities of CAR T cells to prevent target antigen escape as well as mitigate off-target effects. CAR T cells have also been improved by the increased expression of T cell stimulating cytokines to avoid premature T cell exhaustion. Exhaustion can also be avoided by implementing CRISPR-Cas9 technology in CAR T cell manufacturing to perform knock-

in/knock-out reactions of immune checkpoints such as PD1 and CTLA-4 (Dai et al., 2019). These improvements, amongst a myriad of others continuously being researched and discovered, can be employed on a basic, functional C3aR1-targeting CAR construct to provide greater efficacy *in vitro, in vivo,* and in patients.

REFERENCES

Aulestia, F. J., Néant, I., Dong, J., Haiech, J., Kilhoffer, M. C., Moreau, M., & Leclerc, C. (2018). Quiescence status of glioblastoma stem-like cells involves remodeling of Ca2+ signalling and mitochondrial shape. *Scientific Reports, 8*(1), 9731.

Bausart, M., Préat, V., & Malfanti, A. (2022). Immunotherapy for glioblastoma: The promise of combination strategies. *Journal of Experimental & Clinical Cancer Research, 41*(1), 35.

Benavente, F., Piltti, K., Anzalone, A., Di, K., Lakatos, A., Feld, B., David, J., Bui, P., Cummings, B., Bota, D., & Anderson, A. (2022). Complement C3a-C3aR is essential for survival and self-renewal of human neural and glioma stem cells and inhibition prevents glioblastoma growth [Manuscript in preparation].

Bloemberg, D., Nguyen, T., MacLean, S., Zafer, A., Gadoury, C., Gurnani, K., ... & McComb, S. (2020). A high-throughput method for characterizing novel chimeric antigen receptors in jurkat cells. *Molecular Therapy-Methods & Clinical Development, 16*, 238-254.

Bonnet, D., & Dick, J. E. (1997). Human acute myeloid leukemia is organized as a hierarchy that originates from a primitive hematopoietic cell. *Nature Medicine, 3*(7), 730-737.

Brennan, C. W., Verhaak, R. G., McKenna, A., Campos, B., Noushmehr, H., Salama, S. R., ... & Davidsen, T. (2013). *The somatic genomic landscape of glioblastoma. Cell, 155*(2), 462-477.

Brown, C. E., Alizadeh, D., Starr, R., Weng, L., Wagner, J. R., Naranjo, A., ... & Badie, B. (2016). Regression of glioblastoma after chimeric antigen receptor T-cell therapy. *New England Journal of Medicine, 375*(26), 2561-2569.

Cheng, L., Huang, Z., Zhou, W., Wu, Q., Donnola, S., Liu, J. K., ... & Bao, S. (2013). Glioblastoma stem cells generate vascular pericytes to support vessel function and tumor growth. *Cell, 153*(1), 139-152.

Chicaybam, L., Barcelos, C., Peixoto, B., Carneiro, M., Limia, C. G., Redondo, P., ... & Bonamino, M. H. (2017). An efficient electroporation protocol for the genetic modification of mammalian cells. *Frontiers in Bioengineering and Biotechnology, 4*, 99.

Covassin, L., Laning, J., Abdi, R., Langevin, D. L., Phillips, N. E., Shultz, L. D., & Brehm, M. A. (2011). Human peripheral blood CD4 T cell-engrafted non-obese diabetic-scid IL2r γ null H2-Ab1 tm1Gru Tg (human leucocyte antigen D-related 4) mice: a mouse model of human allogeneic graft-versus-host disease*. Clinical & Experimental Immunology, 166*(2), 269-280.

Dai, X., Park, J. J., Du, Y., Kim, H. R., Wang, G., Errami, Y., & Chen, S. (2019). One-step generation of modular CAR-T cells with AAV–Cpf1. *Nature Methods, 16*(3), 247-254.

Davis, M. E. (2016). Glioblastoma: overview of disease and treatment. *Clinical Journal of Oncology Nursing, 20*(5), S2.

Dobes, M., Khurana, V. G., Shadbolt, B., Jain, S., Smith, S. F., Smee, R., ... & Cook, R. (2011). Increasing incidence of glioblastoma multiforme and meningioma, and

decreasing incidence of Schwannoma (2000–2008): findings of a multicenter Australian study. *Surgical Neurology International, 2*.

Dobosz, P., & Dzieciątkowski, T. (2019). The intriguing history of cancer immunotherapy. *Frontiers in Immunology, 2965*.

Dzobo, K., Senthebane, D. A., Ganz, C., Thomford, N. E., Wonkam, A., & Dandara, C. (2020). Advances in therapeutic targeting of cancer stem cells within the tumor microenvironment: an updated review. *Cells, 9*(8), 1896.

Eshhar, Z., Waks, T., Gross, G., & Schindler, D. G. (1993). Specific activation and targeting of cytotoxic lymphocytes through chimeric single chains consisting of antibody-binding domains and the gamma or zeta subunits of the immunoglobulin and T-cell receptors. *Proceedings of the National Academy of Sciences, 90*(2), 720-724.

Finney, H. M., Akbar, A. N., & Lawson, A. D. (2004). Activation of resting human primary T cells with chimeric receptors: costimulation from CD28, inducible costimulator, CD134, and CD137 in series with signals from the TCRζ chain. *The Journal of Immunology, 172*(1), 104-113.

Glantz MJ, Cole BF, Friedberg MH, et al. A randomized, blinded, placebo-controlled trial of divalproex sodium prophylaxis in adults with newly diagnosed brain tumors, *Neurology, 1996, vol. 46 4*(pg. 985-991)

Gross, G., Waks, T., & Eshhar, Z. (1989). Expression of immunoglobulin-T-cell receptor chimeric molecules as functional receptors with antibody-type specificity. *Proceedings of the National Academy of Sciences, 86*(24), 10024-10028.

Haque, W., Thong, Y., Verma, V., Rostomily, R., Butler, E. B., & Teh, B. S. (2020). Patterns of management and outcomes of unifocal versus multifocal glioblastoma. *Journal of Clinical Neuroscience, 74*, 155-159.

Jacinto, F. V., & Esteller, M. (2007). MGMT hypermethylation: a prognostic foe, a predictive friend. *DNA Repair, 6(*8), 1155-1160.

Jayaraman, Jayapriya, et al. "CAR-T design: Elements and their synergistic function." *EBioMedicine 58* (2020): 102931.

Kershaw, M. H., Westwood, J. A., Parker, L. L., Wang, G., Eshhar, Z., Mavroukakis, S. A., ... & Hwu, P. (2006). A phase I study on adoptive immunotherapy using gene-modified T cells for ovarian cancer. *Clinical Cancer Research, 12*(20), 6106-6115.

Kochenderfer, J. N., Wilson, W. H., Janik, J. E., Dudley, M. E., Stetler-Stevenson, M., Feldman, S. A., ... & Rosenberg, S. A. (2010). Eradication of B-lineage cells and regression of lymphoma in a patient treated with autologous T cells genetically engineered to recognize CD19. Blood, *The Journal of the American Society of Hematology, 116*(20), 4099-4102.

Kuwana, Y., Asakura, Y., Utsunomiya, N., Nakanishi, M., Arata, Y., Itoh, S., ... & Kurosawa, Y. (1987). Expression of chimeric receptor composed of immunoglobulin-derived V resions and T-cell receptor-derived C regions. *Biochemical and Biophysical Research Communications, 149*(3), 960-968.

Lan, X., Jörg, D. J., Cavalli, F. M., Richards, L. M., Nguyen, L. V., Vanner, R. J., ... & Dirks, P. B. (2017). Fate mapping of human glioblastoma reveals an invariant stem cell hierarchy. *Nature, 549*(7671), 227-232.

Lathia, J. D., Mack, S. C., Mulkearns-Hubert, E. E., Valentim, C. L., & Rich, J. N. (2015). Cancer stem cells in glioblastoma. *Genes & Development, 29*(12), 1203-1217.

Li, Y., Zhang, Z. X., Huang, G. H., Xiang, Y., Yang, L., Pei, Y. C., ... & Lv, S. Q. (2021). A systematic review of multifocal and multicentric glioblastoma. *Journal of Clinical Neuroscience, 83*, 71-76.

Liau, L. M., Ashkan, K., Tran, D. D., Campian, J. L., Trusheim, J. E., Cobbs, C. S., ... & Bosch, M. L. (2018). First results on survival from a large Phase 3 clinical trial of an autologous dendritic cell vaccine in newly diagnosed glioblastoma. *Journal of Translational Medicine, 16*(1), 1-9.

Maude, S. L., Laetsch, T. W., Buechner, J., Rives, S., Boyer, M., Bittencourt, H., ... & Grupp, S. A. (2018). Tisagenlecleucel in children and young adults with B-cell lymphoblastic leukemia. *New England Journal of Medicine, 378*(5), 439-448.

Malkki, H. (2016). Glioblastoma vaccine therapy disappointment in Phase III trial. *Nature Reviews Neurology, 12*(4), 190-190.

Modrek, A. S., Bayin, N. S., & Placantonakis, D. G. (2014). Brain stem cells as the cell of origin in glioma. *World Journal of Stem Cells, 6*(1), 43.

Moots, P. L., Maciunas, R. J., Eisert, D. R., Parker, R. A., Laporte, K., & Abou-Khalil, B. (1995). The course of seizure disorders in patients with malignant gliomas. *Archives of Neurology, 52*(7), 717-724.

Moritz, D., Wels, W., Mattern, J., & Groner, B. (1994). Cytotoxic T lymphocytes with a grafted recognition specificity for ERBB2-expressing tumor cells. *Proceedings of the National Academy of Sciences, 91*(10), 4318-4322.

Negrin, R. S., & Contag, C. H. (2006). In vivo imaging using bioluminescence: a tool for probing graft-versus-host disease. *Nature Reviews Immunology, 6*(6), 484-490.

Park, J. H., Geyer, M. B., & Brentjens, R. J. (2016). CD19-targeted CAR T-cell therapeutics for hematologic malignancies: interpreting clinical outcomes to date. *Blood, The Journal of the American Society of Hematology*, 127(26), 3312-3320.

Patel, A. P., Tirosh, I., Trombetta, J. J., Shalek, A. K., Gillespie, S. M., Wakimoto, H., ... & Bernstein, B. E. (2014). Single-cell RNA-seq highlights intratumoral heterogeneity in primary glioblastoma. *Science, 344*(6190), 1396-1401.

Poulsen, H. S., Urup, T., Michaelsen, S. R., Staberg, M., Villingshøj, M., & Lassen, U. (2014). The impact of bevacizumab treatment on survival and quality of life in newly diagnosed glioblastoma patients. *Cancer Management and Research, 373-387*.

Prager, B. C., Xie, Q., Bao, S., & Rich, J. N. (2019). Cancer stem cells: the architects of the tumor ecosystem. *Cell Stem Cell, 24*(1), 41-53.

Ravanpay, A. C., Gust, J., Johnson, A. J., Rolczynski, L. S., Cecchini, M., Chang, C. A., ... & Jensen, M. C. (2019). EGFR806-CAR T cells selectively target a tumor-restricted EGFR epitope in glioblastoma. *Oncotarget, 10*(66), 7080.

Rosenberg, S. A., Packard, B. S., Aebersold, P. M., Solomon, D., Topalian, S. L., Toy, S. T., ... & White, D. E. (1988). Use of tumor-infiltrating lymphocytes and

interleukin-2 in the immunotherapy of patients with metastatic melanoma. *New England Journal of Medicine, 319*(25), 1676-1680.

Sampson, J. H., Heimberger, A. B., Archer, G. E., Aldape, K. D., Friedman, A. H., Friedman, H. S., ... & Bigner, D. D. (2010). Immunologic escape after prolonged progression-free survival with epidermal growth factor receptor variant III peptide vaccination in patients with newly diagnosed glioblastoma. *Journal of Clinical Oncology, 28*(31), 4722.

Soda, Y., Marumoto, T., Friedmann-Morvinski, D., Soda, M., Liu, F., Michiue, H., ... & Verma, I. M. (2011). Transdifferentiation of glioblastoma cells into vascular endothelial cells. *Proceedings of the National Academy of Sciences, 108*(11), 4274-4280.

Stupp, R., Mason, W. P., Van Den Bent, M. J., Weller, M., Fisher, B., Taphoorn, M. J., ... & Mirimanoff, R. O. (2005). Radiotherapy plus concomitant and adjuvant temozolomide for glioblastoma. *New England Journal of Medicine, 352*(10), 987-996.

Stupp, R., Hegi, M. E., Mason, W. P., Van Den Bent, M. J., Taphoorn, M. J., Janzer, R. C., ... & Mirimanoff, R. O. (2009). Effects of radiotherapy with concomitant and adjuvant temozolomide versus radiotherapy alone on survival in glioblastoma in a randomised phase III study: 5-year analysis of the EORTC-NCIC trial. *The Lancet Oncology, 10*(5), 459-466.

Tang, X., Zhao, S., Zhang, Y., Wang, Y., Zhang, Z., Yang, M., ... & Zhou, L. (2019). B7-H3 as a novel CAR-T therapeutic target for glioblastoma. *Molecular Therapy-Oncolytics, 14*, 279-287.

Wang, Z., Zhang, H., Xu, S., Liu, Z., & Cheng, Q. (2021). The adaptive transition of glioblastoma stem cells and its implications on treatments. *Signal Transduction and Targeted Therapy, 6*(1), 124.

Weller, M., Butowski, N., Tran, D. D., Recht, L. D., Lim, M., Hirte, H., ... & MacNeil, M. (2017). Rindopepimut with temozolomide for patients with newly diagnosed, EGFRvIII-expressing glioblastoma (ACT IV): a randomised, double-blind, international phase 3 trial. *The Lancet Oncology, 18*(10), 1373-1385.

Xie, X. P., Laks, D. R., Sun, D., Ganbold, M., Wang, Z., Pedraza, A. M., ... & Parada, L. F. (2022). Quiescent human glioblastoma cancer stem cells drive tumor initiation, expansion, and recurrence following chemotherapy. *Developmental Cell, 57*(1), 32-46.

Zanders, E. D., Svensson, F., & Bailey, D. S. (2019). Therapy for glioblastoma: is it working?. *Drug Discovery Today, 24*(5), 1193-1201.

Zola, H., MacArdle, P. J., Bradford, T., Weedon, H., Yasu, H., & Kurosawa, Y. (1991). Preparation and characterization of a chimeric CD 19 monoclonal antibody. *Immunology and Cell Biology , 69*(6), 411-422.